High performance optical absorber based on a plasmonic metamaterial

Jiaming Hao,[1] Jing Wang,[1] Xianliang Liu,[2] Willie J. Padilla,[2] Lei Zhou,[3] and Min Qiu[1,a)]
[1]*Laboratory of Photonics and Microwave Engineering, School of Information and Communication Technology, Royal Institute of Technology (KTH), Electrum 229, Kista, Stockholm 164 40, Sweden*
[2]*Department of Physics, Boston College, 140 Commonwealth Avenue, Chestnut Hill, Massachusetts 02467, USA*
[3]*Department of Physics, Surface Physics Laboratory (State Key Laboratory), Fudan University, Shanghai 200433, People's Republic of China*

(Received 23 March 2010; accepted 8 May 2010; published online 22 June 2010)

High absorption efficiency is particularly desirable at present for various microtechnological applications including microbolometers, photodectors, coherent thermal emitters, and solar cells. Here we report the design, characterization, and experimental demonstration of an ultrathin, wide-angle, subwavelength high performance metamaterial absorber for optical frequencies. Experimental results show that an absorption peak of 88% is achieved at the wavelength of ~1.58 μm, though theoretical results give near perfect absorption. © *2010 American Institute of Physics*. [doi:10.1063/1.3442904]

Metamaterials are artificially structured materials made from arrays of subwavelength "meta-atoms" which can be designed to display fascinating physical properties and promise many potential applications. Much has been investigated, particularly in creating materials with the exotic properties of negative refraction and producing devices for invisibility cloaking.[1–4] To realize such exotic properties requires that designed structures provide specific effective optical constants with low losses. Quite recently, there have been several studies demonstrating metamaterial absorbers,[5–13] in which the loss portions of the optical constants have been sufficiently exploited rather than the real ones. The experimental demonstrations of such effects have, to-date, only been performed at microwave and terahertz frequencies.[5–8]

Here we present the design, characterization, and experimental demonstration of an ultrathin, wide-angle, subwavelength, high performance metamaterial absorber for optical frequencies. Numerical computations show that the near perfect absorption of light can be achieved in very simple metallic nanostructures. The effect is tunable by adjusting the nanostructure dimensions and is almost independent of the angle of incidence. The physical origin of the absorption effect relies on the excitation of localized magnetic and electric dipole resonances. This is different from the idea of using metallic surfaces with spherical nanovoids,[14] due to the excitation of cavity modes. The physical phenomenon is also in sharp contrast to the mechanisms of absorption in nanostructured metallic gratings[15–17] and a dark material made by a low-density carbon nanotube array,[18] in which the high absorbance is the result of the roughness of the surface.

As illustrated in Fig. 1(a), the designed optical metamaterial absorber consists of a layer of gold particles and a gold film, separated by a Al_2O_3 dielectric layer. The thickness of the rectangular metallic particle is denoted by t and its dimensions are W_x and W_y. The thicknesses of the Al_2O_3 dielectric layer and the gold film are represented by d and h, respectively, the lattice constant by a. We first perform numerical computations using the finite-difference-time-domain method[19] to investigate the relationship between the absorption spectrum and the geometric dimensions of nanostructure, and design a perfect absorber with a set of practicable parameters around optical communication wavelengths.

Suppose a plane wave illuminates the structure at normal incidence. Figure 2(a) presents the evolution of the maximum absorption (A) and correspondingly the simulated reflection (R) and transmission (T) as functions of d with other geometric parameters $W_x=W_y=170$ nm, $t=40$ nm, $h=50$ nm, and $a=310$ nm. The resonant absorption peak wavelength (λ_R) corresponding to Fig. 2(a) is shown in Fig. 2(b). The absorbance is calculated using the equation $A=1-R-T$. No higher order diffraction is considered owing to the good subwavelength characterization of the nanostructure [λ_R as shown in Fig. 2(b) is at least 3.9 times larger than the lattice constant of the nanostructure]. There exists an optimal thickness d of the dielectric layer that maximizes the absorption. For the present geometry, when $d=10$ nm, the reflectance vanishes, and the absorbance can be as high as 99% at $\lambda_R=1.55$ μm and has a full width at half maximum of 12%. High absorption is attributed to variation in the near-field plasmon coupling between the gold particle and the continuous gold film. As the dielectric layer thickness increases, the coupling strength increases first until reaching the maximum, then decrease thereafter. When the gold particles are far away from the gold film, the optical properties of such systems are dominantly determined by the film.

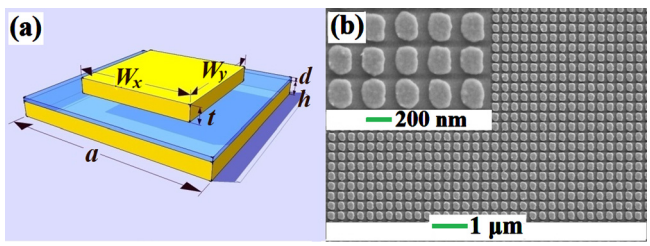

FIG. 1. (Color online) (a) Geometry of the sample studied in this paper. W_x and W_y represent, respectively, the side lengths of rectangular metallic particle along the x and y axis and t represents its thickness. d and h, respectively, denote the thicknesses of the Al_2O_3 dielectric layer and the gold film. a is the lattice constant. (b) Top view SEM image of the fabricated optical metamaterial absorber.

a)Author to whom correspondence should be addressed. Electronic mail: min@kth.se.

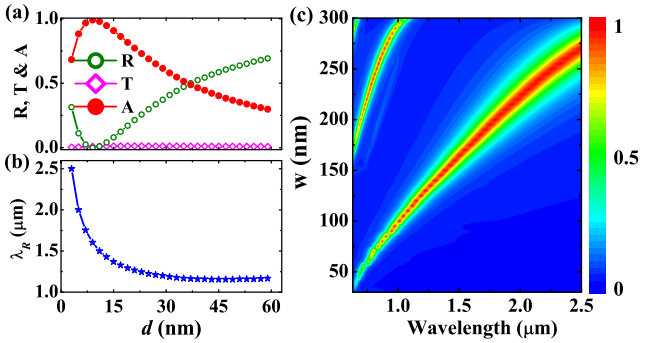

FIG. 2. (Color online) (a) The maximum absorption (A) and correspondingly simulated reflection (R) and transmission (T) spectra as functions of the thickness of dielectric layer d with other geometric parameters $W_x = W_y = 170$ nm, $t = 40$ nm, $h = 50$ nm, and $a = 310$ nm. (b) The resonant absorption peak wavelength (λ_R) corresponding to (a) as a function of d; (c) absorbance as a function of wavelength and the width of the metallic particle, where $W_x = W_y = W$, $t = 40$ nm, $d = 10$ nm, $h = 50$ nm, and $a = 310$ nm.

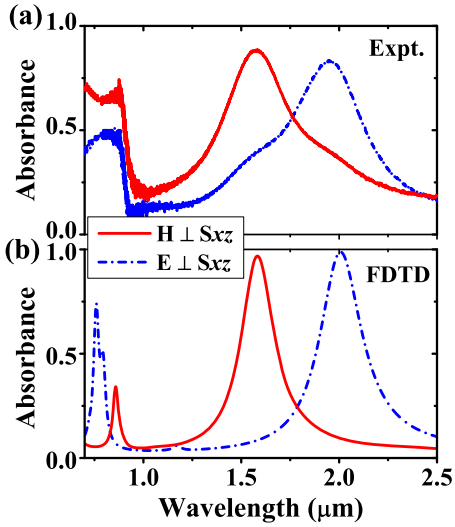

FIG. 3. (Color online) Measured (a) and simulated (b) absorbance spectra for a sample with $W_x = 170$ nm, $W_y = 230$ nm, $t = 40$ nm, $d = 10$ nm, $h = 50$ nm, and $a = 310$ nm at 20° angle of incidence.

These results are qualitatively consistent with previous works.[20,21]

Dependences of the absorbance on wavelength and widths of the gold particle ($W_x = W_y = W$) for $t = 40$ nm, $d = 10$ nm, $h = 50$ nm, and $a = 310$ nm are shown in Fig. 2(c). One can observe that the resonant absorption wavelength can be altered over a broad spectral range by changing the width of the gold particle. As W increases, the total absorption spectrum is redshifted. This is due to the increase in the effective resonance wavelength. In comparison with $W = 170$ nm, when $W = 230$ nm(300 nm), λ_R shifts to 2.05 μm (3.15 μm, not shown) while the absorbance is 99% (97%).

The sensitivity of the absorption peak to the thickness of gold particle t, the thickness of gold film h, and the refractive index of the dielectric layer n_d, are also investigated. For further details, please refer to the supplementary material.[27]

In our experiments, the multilayered metamaterial absorber was fabricated on a quartz substrate with standard microfabrication techniques. Figure 1(b) shows a scanning electron microscopy (SEM) image of a fabricated metamaterial absorber with the dimensions $W_x = 170$ nm, $W_y = 230$ nm, $t = 40$ nm, $d = 10$ nm, $h = 50$ nm, and $a = 310$ nm. The side lengths along different axis are not equal, and consequently, λ_R different for TE and TM polarized light. For example, when the magnetic field (H) of the incident light is set perpendicular to the plane of incidence $S_{xz}(S_{yz})$, the effective resonant wavelength is determined by the side length $W_x(W_y)$. Figure 3(a) presents the experimental absorbance as a function of wavelength for differential polarizations of incident radiation, which is calculated from the measured transmission and reflection. For TM ($H \perp S_{xz}$) case, the maximum absorption of 88% is obtained at the wavelength 1.58 μm. For the case of TE ($E \perp S_{xz}$) radiation as shown in Fig. 3(a) by the dashed dotted line, the maximum absorption can be as high as 83% and λ_R is shifted to 1.95 μm. Numerical simulations were carried out for this metamaterial structure and are plotted in Fig. 3(b) in comparison to experimental data. Very good agreements are found between the numerical and experimental results. For example, both the simulated and experimental absorbencies reach a maximum at the wavelength 1.58 μm for $H \perp S_{xz}$ case, although experimentally, the maximum is 88%, less than the simulated value of 97%. Disagreement stems from broadening of the experimental absorption, which originates from fabricational tolerances of the side length.

For this type of metamaterial absorber, the absorption effect is robust for non-normal incident angles. Further simulations are performed to verify this effect with the dimensions similar to the experimental fabricated one. The simulated absorbencies as functions of wavelength and the angle of incidence are presented in Fig. 4 for different polarizations of incident light. For the TE polarization $E \perp S_{yz}$ case [Fig. 4(a)], when the angle of incidence is up to 65° (75°), although the bandwidth becomes slightly narrower, the maximum absorption remains 90% (73%). For the TM polarization $H \perp S_{yz}$ case [Fig. 4(b)], the maximum absorption remains greater than 80% even for the angle of 80°. The details of two other cases are listed in the figure caption.

To reveal the physical origin of the absorption in our metamaterial, the electromagnetic field distributions for the

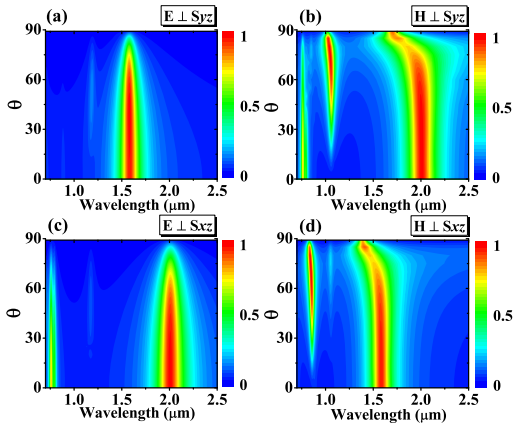

FIG. 4. (Color online) Absorbance as a function of wavelength and the angle of incidence for different polarization incident radiations, where $W_x = 170$ nm, $W_y = 230$ nm, $t = 40$ nm, $d = 10$ nm, $h = 50$ nm, and $a = 310$ nm. (a) $E \perp S_{yz}$, when the angle of incidence is up to 65° (75°), the maximum absorption remains 90% (73%); (b) $H \perp S_{yz}$, the maximum absorption remains greater than 80% even for the angle of 80°; (c) $E \perp S_{xz}$, for incident angle to 55° (65°), the maximum absorption is 90% (80%); (d) $H \perp S_{xz}$, for incident angle 80°, the maximum absorption remains 80%, the center wavelength decreases by 0.12 μm.

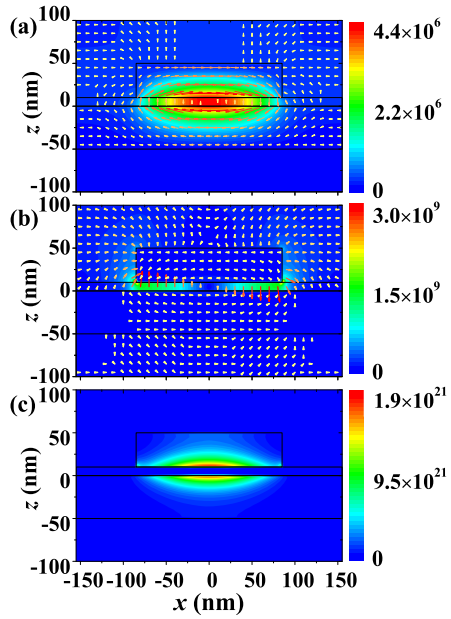

FIG. 5. (Color online) (a) The colormap represents the amplitude of magnetic field (H_y) and the arrows represent the electric displacement; (b) the colormap represents the amplitude of electric field (E_x and E_z) and the arrows denote the electric field polarization; (c) resistive heating; for incidence light with the wavelength 1.55 μm, $H \perp S_{xz}$ polarization at the normal incidence, where $W_x = W_y = 170$ nm, $t = 40$ nm, $d = 10$ nm, $h = 50$ nm, and $a = 310$ nm.

resonant modes are investigated. For example, Fig. 5(a) illustrates the magnetic field and electric displacement distributions for an absorber with $W_x = W_y = 170$ nm, $t = 40$ nm, $d = 10$ nm, $h = 50$ nm, and $a = 310$ nm at the wavelength 1.55 μm, which are calculated by the commercial COMSOL MULTIPHYSICS software based on the three-dimensional finite elements method. A plane wave with polarization $H \perp S_{xz}$ is normally illuminated on the structure. The electric displacement vectors represented by the arrows in both the gold particle and the gold film are opposite to each other,[22] which generates a significant magnetic response[23,24] as shown in Fig. 5(a) denoted by surface colormap. The electric field distributions for this structure are plotted in Fig. 5(b). It is found that there exists strong electric dipole resonances resulting from charges accumulated at the sides of gold particle which couple to their image charges in the gold surface. The absorption effect is thus due to the excitation of localized magnetic and electric dipole resonances. (This is also evidenced by the extracted effective electromagnetic parameters, see supplementary material Fig. S1.[27]) Such strong resonances effectively trap light energy and provide sufficient time to dissipate it by the Ohmic losses within the metals (Al_2O_3 is lossless in this wavelength regime). To further comprehend this point, the time averaged resistive heating (Q) generated by the structure is investigated as shown in Fig. 5(c), which is calculated using $Q = (1/2)\varepsilon_0 \omega \, \mathrm{Im}\, \varepsilon_{\mathrm{Au}}(\omega) |\mathrm{E}|^2$.[25,26] In our simulations, the temperature effect on the material properties has been ignored. Suppose the average rate of energy transport by the incident radiation is 1 W. The calculated results show that the time averaged power dissipation caused by the gold particle and the gold film are, respectively, 0.628 W and 0.362 W, except for approximately 1% of the energy which passes through the structure. This is different from the studies of microwave and terahertz metamaterial absorbers, in which the absorptions arise mainly due to dielectric losses.[5–8]

The whole thickness of the perfect optical metamaterial absorber is extremely thin, only 100 nm, which is 15 times shorter than the resonant absorption peak wavelength. The high performance absorption is almost independent of incident angle and can be manipulated by adjusting the nanostructure dimensions. Furthermore, the optical absorber has a very simple geometrical structure and it is easy to be integrated into complex photonic devices. The present absorber can also tailor the thermal or optical responses to radiation covering, in principle, any targeted region of the electromagnetic spectrum. Supplementary materials are available for details of sample designation, fabrication, and measurement.[27]

This work was supported by the Swedish Foundation for Strategic Research (SSF) and the Swedish Research Council (VR). L.Z. was supported by the NSFC (Grant Nos. 60725417 and 60990321), China-973 Project (Grant No. 2006CB921506), and Shanghai Science and Technology Committee. J.M.H. and J.W. contributed equally to this work.

[1] D. R. Smith, W. J. Padilla, D. C. Vier, S. C. Nemat-Nasser, and S. Schultz, Phys. Rev. Lett. **84**, 4184 (2000).
[2] D. R. Smith, J. B. Pendry, and M. C. K. Wiltshire, Science **305**, 788 (2004).
[3] U. Leonhardt, Science **312**, 1777 (2006).
[4] J. B. Pendry, D. Schurig, and D. R. Smith, Science **312**, 1780 (2006).
[5] N. I. Landy, S. Sajuyigbe, J. J. Mork, D. R. Smith, and W. J. Padilla, Phys. Rev. Lett. **100**, 207402 (2008).
[6] N. I. Landy, C. M. Bingham, T. Tyler, N. Jokerst, D. R. Smith, and W. J. Padilla, Phys. Rev. B **79**, 125104 (2009).
[7] H. Tao, N. I. Landy, C. M. Bingham, X. Zhang, R. D. Averitt, and W. J. Padilla, Opt. Express **16**, 7181 (2008).
[8] H. Tao, C. M. Bingham, A. C. Strikwerda, D. Pilon, D. Shrekenhamer, N. I. Landy, K. Fan, X. Zhang, W. J. Padilla, and R. D. Averitt, Phys. Rev. B **78**, 241103(R) (2008).
[9] M. Diem, T. Koschny, and C. M. Soukoulis, Phys. Rev. B **79**, 033101 (2009).
[10] Y. Avitzour, Y. A. Urzhumov, and G. Shvets, Phys. Rev. B **79**, 045131 (2009).
[11] C. Wu, Y. Avitzour, and G. Shvets, Proc. SPIE **7029**, 70290W (2008).
[12] C. Argyropoulos, E. Kallos, Y. Zhao, and Y. Hao, Opt. Express **17**, 8467 (2009).
[13] N. Jack, H. Y. Chen, and C. T. Chan, Opt. Lett. **34**, 644 (2009).
[14] T. V. Teperik, F. J. Abajo, A. G. Borisov, M. Abdelsalam, P. N. Bartlett, Y. Sugawara, and J. J. Baumberg, Nat. Photonics **2**, 299 (2008).
[15] J. Le Perchec, P. Quémerais, A. Barbara, and T. López-Ríos, Phys. Rev. Lett. **100**, 066408 (2008).
[16] V. G. Kravets, F. Schedin, and A. N. Grigorenko, Phys. Rev. B **78**, 205405 (2008).
[17] E. Popov, D. Maystre1, R. C. McPhedran, M. Nevière, M. C. Hutley, and G. H. Derrick, Opt. Express **16**, 6146 (2008); E. Popov, S. Enoch, and N. Bonod, *ibid.* **17**, 6770 (2009).
[18] Z. P. Yang, L. J. Ci, J. A. Bur, S. Y. Lin, and P. M. Ajayan, Nano Lett. **8**, 446 (2008).
[19] A. Taflove, *Computational Electrodynamics: The Finite-Difference-Time-Domain Method* (Artech House, Norwood, 2000).
[20] W. R. Holland and D. G. Hall, Phys. Rev. Lett. **52**, 1041 (1984).
[21] G. Lévêque and O. J. F. Martin, Opt. Lett. **31**, 2750 (2006).
[22] In the areas above the gold particle and below the gold film, the electric displacement is not zero, but much smaller than the electric displacement in the resonance region.
[23] U. K. Chettiar, A. V. Kildishev, T. A. Klar, and V. M. Shalaev, Opt. Express **14**, 7872 (2006).
[24] H. K. Yuan, U. K. Chettiar, W. S. Cai, A. V. Kildishev, A. Boltasseva, V. P. Drachev, and V. M. Shalaev, Opt. Express **15**, 1076 (2007).
[25] J. D. Jackson, *Classical Electrodynamics*, 3rd ed. (Wiley, New York, 1999).
[26] R. Ruppin, Phys. Lett. A **299**, 309 (2002).
[27] See supplementary material at http://dx.doi.org/10.1063/1.3442904 for details of sample designation, fabrication, and measurement.